

We are IntechOpen, the world's leading publisher of Open Access books Built by scientists, for scientists

6,900

Open access books available

186,000

International authors and editors

200M

Downloads

Our authors are among the

154

Countries delivered to

TOP 1%

most cited scientists

12.2%

Contributors from top 500 universities



WEB OF SCIENCE™

Selection of our books indexed in the Book Citation Index
in Web of Science™ Core Collection (BKCI)

Interested in publishing with us?
Contact book.department@intechopen.com

Numbers displayed above are based on latest data collected.
For more information visit www.intechopen.com



Ligand-Protected Gold Clusters

Sakiat Hossain, Lakshmi V. Nair, Junta Inoue,
Yuki Koyama, Wataru Kurashige and Yuichi Negishi

Additional information is available at the end of the chapter

<http://dx.doi.org/10.5772/intechopen.73441>

Abstract

Small gold clusters with diameters less than or equal to 2 nm (below approximately 200 atoms) possess geometric and electronic structures different from bulk gold. When these gold clusters are protected by ligands, these clusters can be treated as chemical compounds. This review focuses on gold clusters protected by chalcogenate (thiolate, selenolate, or tellurolate) ligands and describes the methods by which these clusters are synthesized as well as their geometric/electronic structures and physical and chemical properties. Recent findings regarding ligand exchange reactions, which may be used to impart functionality to these compounds, are also described.

Keywords: gold clusters, chalcogenate, geometric and electronic structures, physical and chemical properties, ligand exchange reactions

1. Introduction

Small gold clusters with diameters less than or equal to 2 nm (below approximately 200 atoms) possess geometric and electronic structures different from those of bulk gold [1]. The geometric structure often consists of an atomic arrangement, such as an icosahedral structure, that differs from the close-packed structure of bulk gold, as a result of reducing the surface energy. In addition, a discrete electronic structure appears rather than the continuous structure observed in the bulk element. Owing to these characteristics, small gold clusters exhibit fundamental properties and functionalities different from those of bulk gold. In addition, when these gold clusters are protected by ligands, it is possible to treat them as chemical compounds. In early

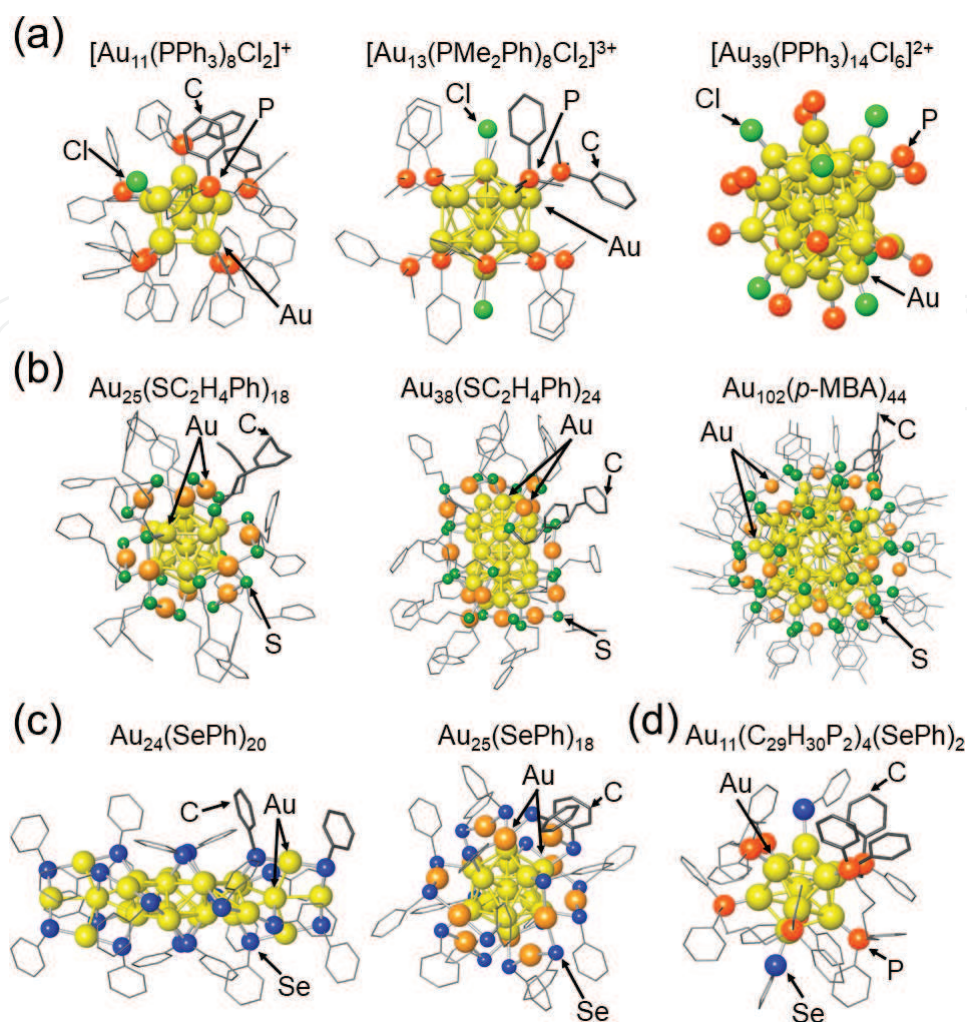


Figure 1. The crystal structures of (a) $Au_n(PR_3)_m$, (b) $Au_n(SR)_m$, (c) $Au_n(SeR)_m$, and (d) $Au_n(PR_3)_m(SeR)_l$. H atoms are omitted for clarity. In $[Au_{39}(PPh_3)_{14}Cl_6]^{2+}$, C atoms are also not shown (these figures were adapted from Refs. [2, 10, 11, 29, 30, 34, 47, 48, 59]).

studies, beginning in the 1960s, phosphine was employed as a protective ligand [2–16]. Representative phosphine (PR_3)-protected gold clusters ($Au_n(PR_3)_m$) include $[Au_{11}(PPh_3)_8Cl_2]^+$, $[Au_{13}(PMe_2Ph)_8Cl_2]^{3+}$, $[Au_{39}(PPh_3)_{14}Cl_6]^{2+}$, and $Au_{55}(PPh_3)_{12}Cl_6$ (**Figure 1(a)**). Unfortunately, these clusters have been found to be unstable in solution, which restricts their practical applications. In contrast, thiolate (SR)-protected gold clusters ($Au_n(SR)_m$), first synthesized by Brust et al. in 1994 (**Figure 1(b)**) [17], are highly stable both in solution and in the solid state, because the SR ligands form strong bonds with gold atoms. These $Au_n(SR)_m$ clusters exhibit various physical and chemical properties not shown by bulk gold, such as photoluminescence and catalytic activity. For these reasons, SR ligands have become the most common choice for use with gold clusters [18–40]. Recently, the synthesis of gold clusters protected by other chalcogenates (selenolate (SeR) or tellurolate (TeR); **Figure 1(c)**) [41–51], by alkynes [52–54], or by two kinds of ligand (**Figure 1(d)**) [55–59] has also been reported. In this chapter, we focus on gold clusters protected by chalcogenates ($Au_n(XR)_m$; $XR = SR, SeR, \text{ or } TeR$) and describe the synthetic procedures, geometric/electronic structures, and physical and chemical properties of these gold clusters. Moreover, the physical and chemical properties of these gold clusters are greatly affected by the type of functional group of the protecting ligand. The ligand exchange

reaction is a very powerful means for introducing the different ligands into the pre-synthesized cluster. Although this type of reaction was discovered nearly 20 years ago [60–65], the associated mechanism was not fully understood at that time. Recently, tremendous progress has been made in terms of the precise synthesis and evaluation of metal clusters, and details of these reactions have been elucidated [66, 67]. Recent findings regarding these reactions are therefore also included herein.

2. Synthesis of $Au_n(XR)_m$ clusters

The method used most frequently to synthesize $Au_n(XR)_m$ clusters is based on the chemical reduction of gold ions in the presence of ligands in solution (**Figure 2**). In this approach, a gold salt and the ligand are mixed in solution to form Au-ligand complexes that are subsequently treated with a reducing agent (normally $NaBH_4$). $Au_n(XR)_m$ clusters are formed by the aggregation

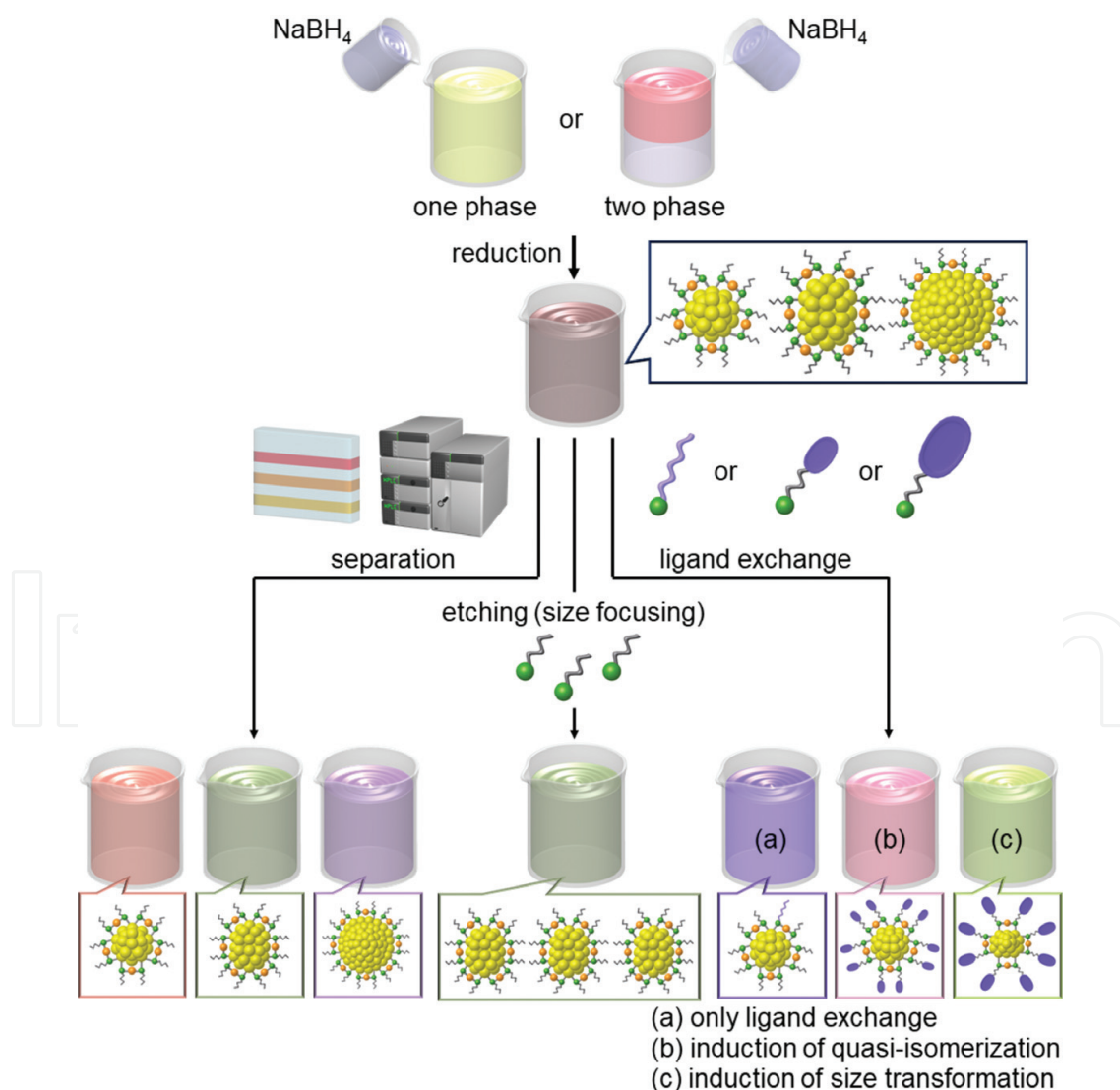


Figure 2. A typical procedure for the synthesis of $Au_n(SR)_m$ clusters having a well-defined chemical composition.

of the resulting gold atoms in conjunction with surface protection by the ligands [18]. In the first report published by Brust et al., dodecanethiolate was used as the ligand [17]. Because a gold salt and dodecanethiolate are soluble in different solvents, Brust transferred the gold salt from an aqueous phase to a ligand-containing toluene phase using a phase-transfer reagent (representing a two-phase system; **Figure 2**). In contrast, in more recent research, tetrahydrofuran (THF) has often been used as the solvent because it could dissolve both gold salt and ligand [68]. This removes the need for phase transfer of the gold salt and thereby simplifies the synthesis to a one-phase system (**Figure 2**). Similarly, when a hydrophilic thiol is used as the ligand, gold clusters can be synthesized in a one-phase system [69–71].

The product obtained from this technique is typically a mixture of $Au_n(XR)_m$ clusters having various numbers of constituent atoms. Because the physical and chemical properties of the clusters are greatly affected by the number of atoms, separation by size or conversion to stable clusters by exposure to severe conditions is required to obtain $Au_n(XR)_m$ clusters with well-defined physical properties and functions (**Figure 2**) [18, 72]. Polyacrylamide gel electrophoresis [69–72], high-performance liquid chromatography [72–77], and solvent extraction are the most frequently applied techniques for size separation. It is also common to use an etching reaction for size convergence [72, 78–82]. In addition to these techniques, the ligand exchange method, in which the ligands of a specific $Au_n(XR)_m$ cluster are replaced with other ligands, is an effective means of generating $Au_n(XR)_m$ clusters with a specific chemical composition (**Figure 2**) [83]. Recent results associated with such ligand exchange reactions are discussed in Section 6.

3. Geometrical structures of $Au_n(XR)_m$ clusters

Until 2007, it was believed that $Au_n(SR)_m$ clusters possess a geometrical structure in which an Au core is covered with thiolate ligands (**Figure 3(a)**) [84]. Since then, single-crystal X-ray

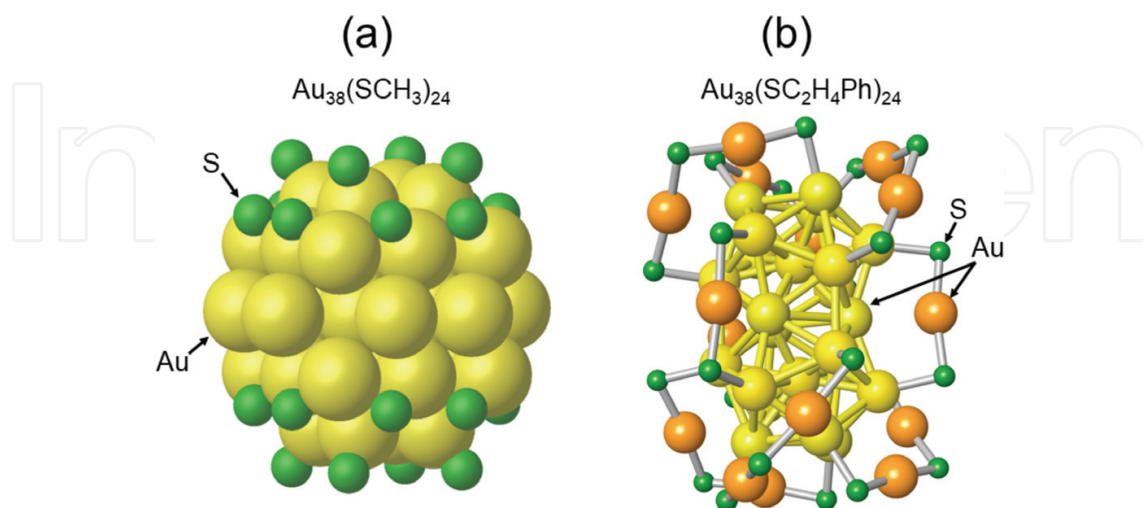


Figure 3. The geometrical structures of $Au_{38}(SR)_{24}$ (a) predicted by theoretical calculations in 1999 and (b) determined by single-crystal X-ray structural analysis in 2010. The R groups have been omitted for clarity (these figures were adapted from Refs. [30, 84]).

structural analysis has revealed that several $\text{Au}_n(\text{SR})_m$ clusters consist of an Au core covered with multiple $-\text{S}(\text{R})[-\text{Au}-\text{S}(\text{R})]_x-$ staples (**Figure 3(b)**) [30, 85–88]. Based on the geometrical structures determined for $\text{Au}_n(\text{SR})_m$ clusters to date, it can be assumed that almost all small $\text{Au}_n(\text{SR})_m$ clusters have this type of core-shell structure. Single-crystal X-ray structural analysis has also demonstrated that small $\text{Au}_n(\text{SeR})_m$ clusters have core-shell structures similar to those of small $\text{Au}_n(\text{SR})_m$ clusters (**Figure 1(c)**) [47, 48]. The geometrical structure of $\text{Au}_n(\text{TeR})_m$ clusters has not yet been determined experimentally, although theoretical calculations [45, 89] have shown that these clusters are also likely to have a similar core-shell structure.

4. Electronic structures of $\text{Au}_n(\text{XR})_m$ clusters

Unlike bulk gold, small $\text{Au}_n(\text{SR})_m$ clusters have discrete electronic structures. As a result, multiple peak structures can be observed in the optical absorption spectra of these clusters. As an example, $\text{Au}_n(\text{SC}_{12}\text{H}_{25})_m$ clusters show multiple peak structures across the entire visible range in their optical absorption spectra up to the size of $\text{Au}_{144}(\text{SC}_{12}\text{H}_{25})_{60}$ (**Figure 4**) [75]. Such fine peak structures are not observed in the spectra of larger clusters, although peaks that can be attributed to surface plasmon resonance absorption have been identified at approximately

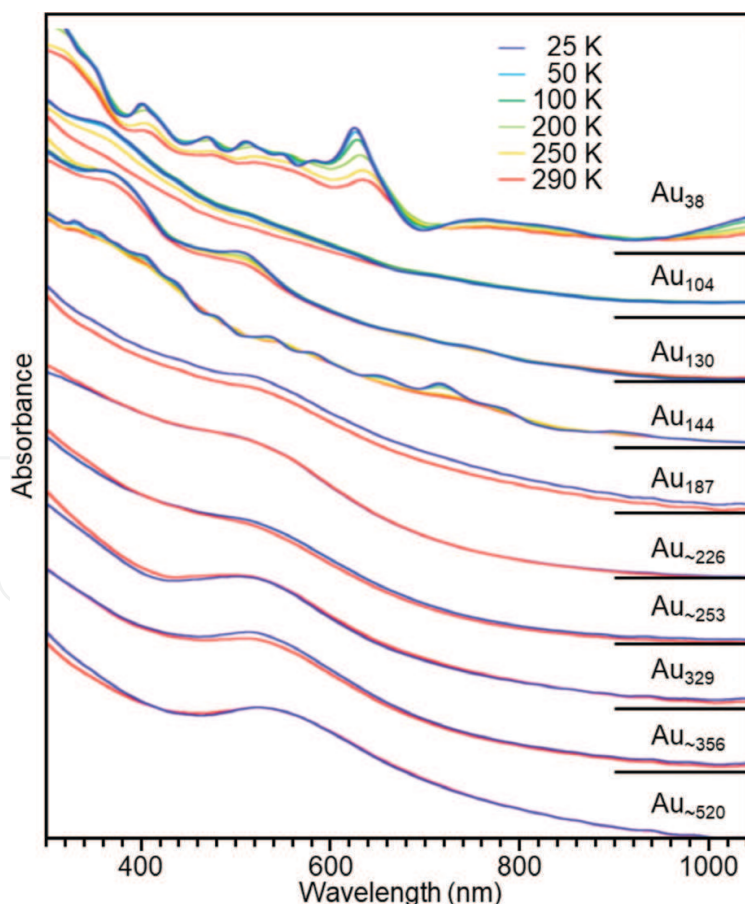


Figure 4. Optical absorption spectra of films composed of $\text{Au}_n(\text{SC}_{12}\text{H}_{25})_m$ clusters ($n = 38\text{--}520$) at various temperatures (25–290 K) (this figure was adapted from Ref. [75]).

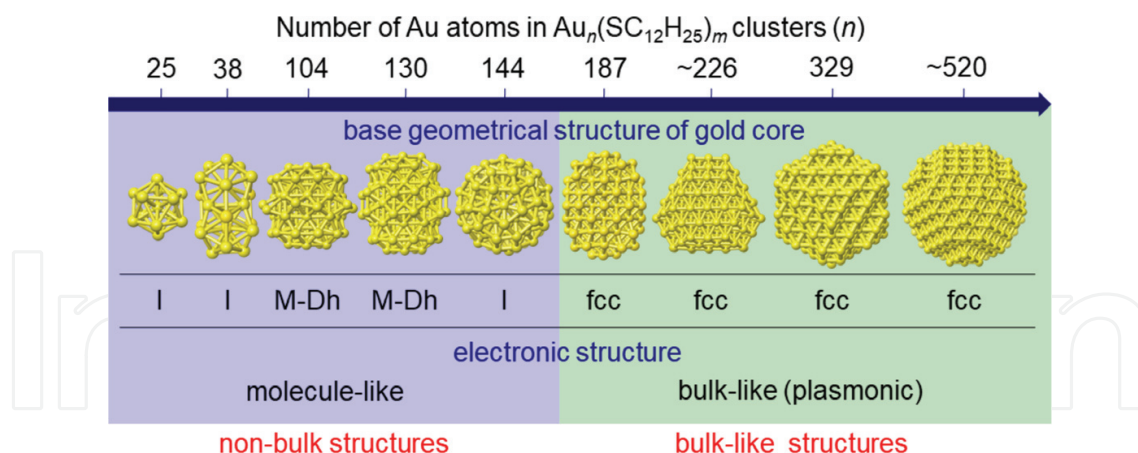


Figure 5. Structural changes in $\text{Au}_n(\text{SC}_{12}\text{H}_{25})_m$ clusters with varying numbers of gold atoms (this figure was adapted from Ref. [75]).

520 nm in their optical absorption spectra (**Figure 4**). Thus, the electronic structures of $\text{Au}_{187}(\text{SC}_{12}\text{H}_{25})_{68}$ and larger clusters tend to resemble that of bulk gold (**Figure 5**) [75].

At present, the relationship between cluster size and electronic structure is not well understood for $\text{Au}_n(\text{SeR})_m$ and $\text{Au}_n(\text{TeR})_m$ clusters, because only a small number of such compounds have been studied to date. However, the researches regarding $\text{Au}_{25}(\text{SeR})_{18}$ and $\text{Au}_{38}(\text{SeR})_{24}$ clusters have demonstrated that changing the ligands from SR to SeR reduces the HOMO-LUMO gap of the clusters [42, 43] and that this effect becomes more pronounced in the case of clusters containing TeR in the ligand shell [45].

5. Physical and chemical properties of $\text{Au}_n(\text{XR})_m$ clusters

$\text{Au}_n(\text{SR})_m$ clusters exhibit size-specific electronic structures, and their physical and chemical properties also vary with size. Herein, we first discuss typical physical and chemical characteristics of such $\text{Au}_n(\text{SR})_m$ clusters.

5.1. Photoluminescence

Small $\text{Au}_n(\text{SR})_m$ clusters have been shown to exhibit photoluminescence (**Figure 6(a)**) [18, 20, 23, 70, 71, 90]. As an example, $\text{Au}_{25}(\text{SG})_{18}$ (SG = glutathionate) exhibits photoluminescence with an estimated quantum yield of $\sim 1 \times 10^{-3}$ [71], which can be used for sensing and imaging applications [91].

5.2. Redox behavior

$\text{Au}_n(\text{SR})_m$ clusters also display redox behavior [20, 21]. **Figure 6(b)** shows a differential pulse voltammogram obtained from $\text{Au}_{25}(\text{SC}_2\text{H}_4\text{Ph})_{18}$, in which the peaks at -1.9 and -0.3 V originate from $[\text{Au}_{25}(\text{SC}_2\text{H}_4\text{Ph})_{18}]^{-/2-}$ and $[\text{Au}_{25}(\text{SC}_2\text{H}_4\text{Ph})_{18}]^{0/-}$ redox couples, respectively. This

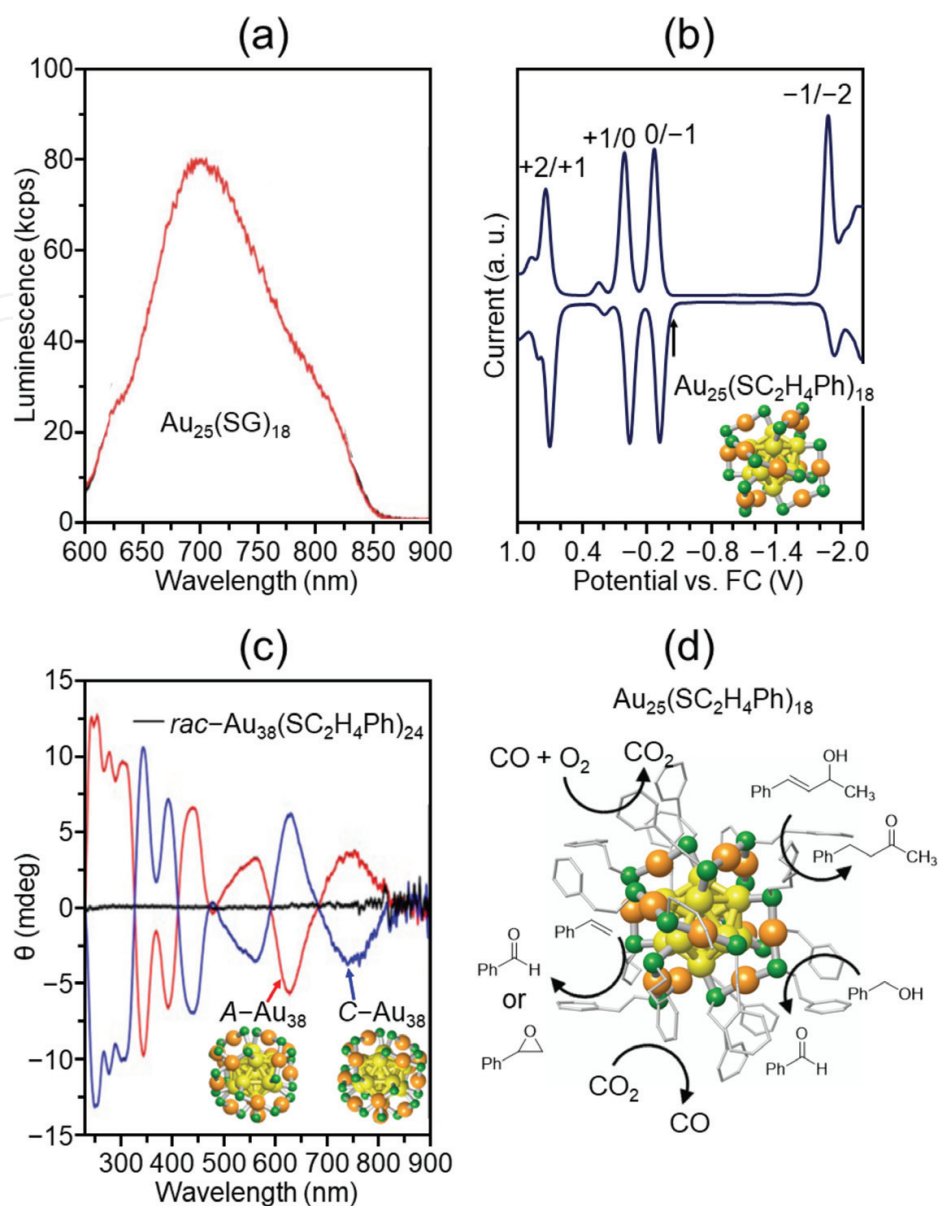


Figure 6. Size-specific physical and chemical properties of $Au_n(SR)_m$ clusters: (a) photoluminescence, (b) redox behavior, (c) optical activity, and (d) catalytic activity (these figures were adapted from Refs. [22, 90, 95]).

redox behavior is not confined to clusters with discrete electronic structures; $Au_n(SR)_m$ clusters larger than $Au_{144}(SR)_{60}$ also exhibit redox behavior as a result of quantized double-layer charging [21]. The redox properties of $Au_n(SR)_m$ clusters could be applied to single-electron transistors [92].

5.3. Optical activity

Several clusters, such as $Au_{38}(SR)_{24}$ and $Au_{40}(SR)_{24}$, have optical isomers with different $-S(R)[-Au-S(R)]_x-$ staple ($x = 1, 2$) configurations [93–95] and thus are optically active [36]. **Figure 6(c)** presents the circular dichroism spectra of two optical isomers of $Au_{38}(SC_2H_4Ph)_{24}$

[95]. The anisotropy factor associated with the optical activity of this cluster increases with wavelength up to a maximum of 4×10^{-3} .

5.4. Catalytic activity

Catalytic activity is another typical size-specific property of $\text{Au}_n(\text{SR})_m$ clusters (**Figure 6(d)**) [22, 72]. As an example, $\text{Au}_{25}(\text{SR})_{18}$ catalyzes the oxidation of CO, styrene, benzyl alcohol, cyclohexane, and sulfides. The same cluster also exhibits catalytic activity for the hydrogenation of nitrophenol, aldehydes, and ketones and promotes C—C coupling reactions. As noted, several $\text{Au}_n(\text{SR})_m$ clusters have optical isomers and therefore could potentially function as asymmetric catalysts [96].

5.5. Effect of changing ligands

Regarding $\text{Au}_n(\text{SeR})_m$ and $\text{Au}_n(\text{TeR})_m$ clusters, it has been reported that the incorporation of SeR or TeR ligands changes the nature of the bonding between the Au atoms and the ligands [97, 98]. In the case of $\text{Au}_n(\text{SeC}_{12}\text{H}_{25})_m$ clusters, this effect reduces the degree of charge transfer from the Au atoms to the ligands (**Figure 7(a)**) such that the Au—ligand bond becomes much more covalent than that in $\text{Au}_n(\text{SC}_{12}\text{H}_{25})_m$ clusters [41]. Owing to these changes in bonding characteristics, $\text{Au}_{25}(\text{SeR})_{18}$ ($\text{R} = \text{C}_{12}\text{H}_{25}$ or C_8H_{17}) exhibits greater resistance to degradation in solution compared with $\text{Au}_{25}(\text{SR})_{18}$ ($\text{R} = \text{C}_{12}\text{H}_{25}$ or C_8H_{17}) (**Figure 7(b)**) [42, 99]. In addition to such an improved stability, the use of SeR ligands is expected to improve conductivity between the gold core and the ligands [97, 100, 101], and future work is likely to demonstrate the conductivity of $\text{Au}_n(\text{SeR})_m$ clusters. Furthermore, recent studies have found that $\text{Au}_{25}(\text{SePh})_{18}$ exhibits catalytic activity for the reduction of 4-nitrophenol (**Figure 7(c)**) [48].

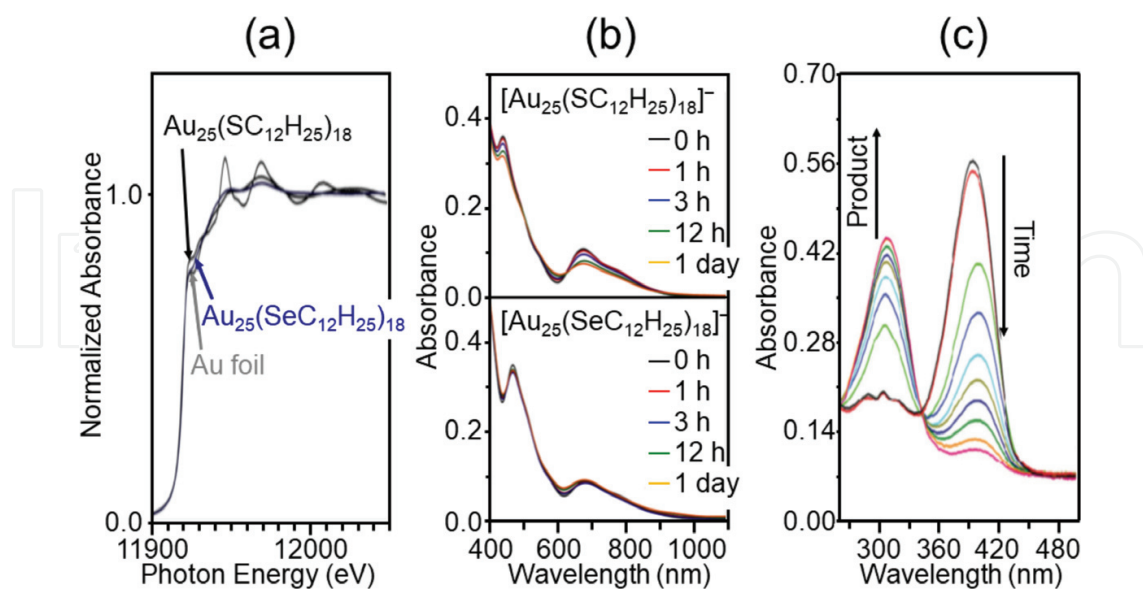


Figure 7. A comparison of (a) the Au L_3 -edge X-ray absorption near-edge structure spectra of $\text{Au}_{25}(\text{SeC}_{12}\text{H}_{25})_{18}$ and $\text{Au}_{25}(\text{SC}_{12}\text{H}_{25})_{18}$ and (b) the stability of $\text{Au}_{25}(\text{SeC}_{12}\text{H}_{25})_{18}$ and $\text{Au}_{25}(\text{SC}_{12}\text{H}_{25})_{18}$ in solution under harsh conditions. (c) Representative UV-vis optical absorption spectra acquired during the reduction of 4-nitrophenol to 4-aminophenol over $\text{Au}_{25}(\text{SePh})_{18}$ (these figures were adapted from Refs. [42, 43, 48]).

6. Ligand exchange reactions

As described above, $Au_n(SR)_m$ clusters tend to resist degradation. However, this type of metal cluster readily exchanges its ligands with other coexisting ligands in solution (**Figure 8(a)**). A complete understanding of the associated mechanism would allow these reactions to be controlled, thus permitting synthesis of novel metal clusters with specific functions. Recently, more details regarding exchange reactions between metal clusters and ligands have been reported, and these findings are discussed in this section.

6.1. Mechanism

Murray et al. reported the ligand exchange reactions of this type of cluster nearly 20 years ago [60–65]. However, their research was conducted using mixtures and did not use advanced techniques such as mass spectrometry and single-crystal X-ray structural analysis to characterize the products. Therefore, a thorough understanding of the details of these reactions was not obtained. More recent research has elucidated the associated mechanism. As an example, $Au_{25}(SR)_{18}$ has a geometry in which the Au_{13} core is covered by six $-S(R)-[Au-S(R)]_2-$ staples (**Figure 9(a)**). As a result, there are two types of SR units in $Au_{25}(SR)_{18}$: those in contact with the Au_{13} core (core-site SR; **Figure 9(a)**) and those at the apex of each staple (apex-site SR; **Figure 9(a)**) [102, 103]. Ackerson et al. performed a single-crystal X-ray structural analysis of the product obtained from the reaction of $Au_{25}(SC_2H_4Ph)_{18}$ ($SC_2H_4Ph = 2$ -phenyl ethanethiolate)

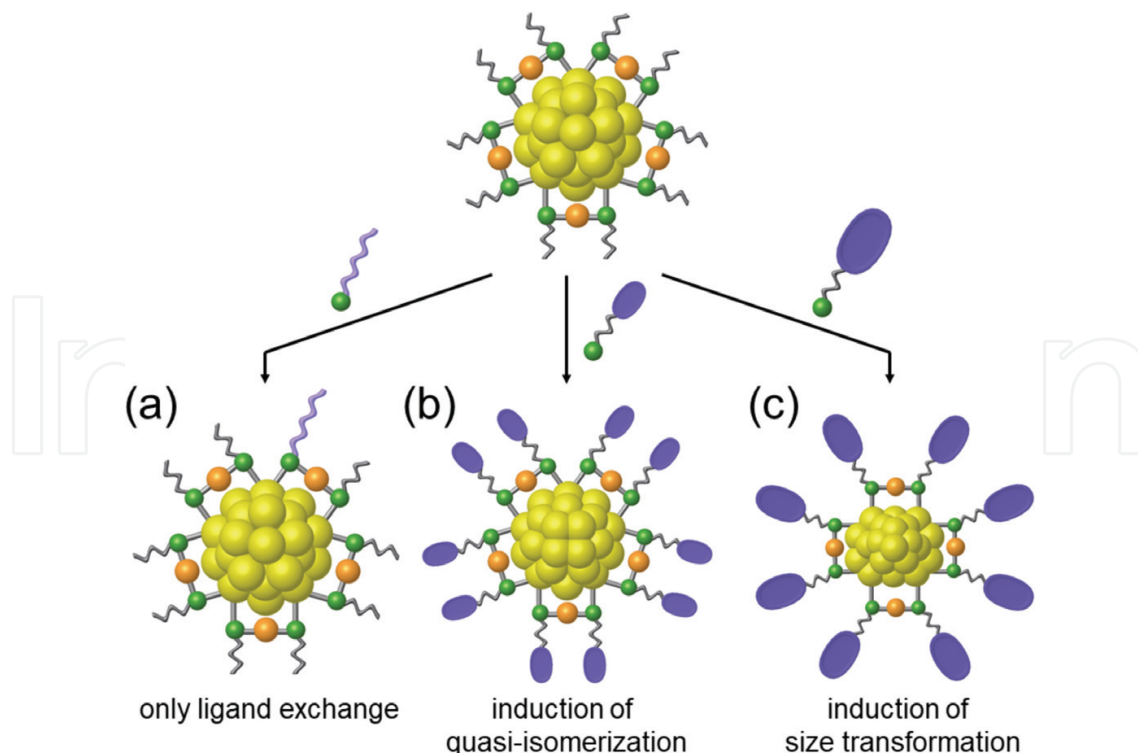


Figure 8. A schematic diagram of ligand exchange reactions including (a) only ligand exchange, (b) induction of quasi-isomerization, and (c) induction of size transformation.

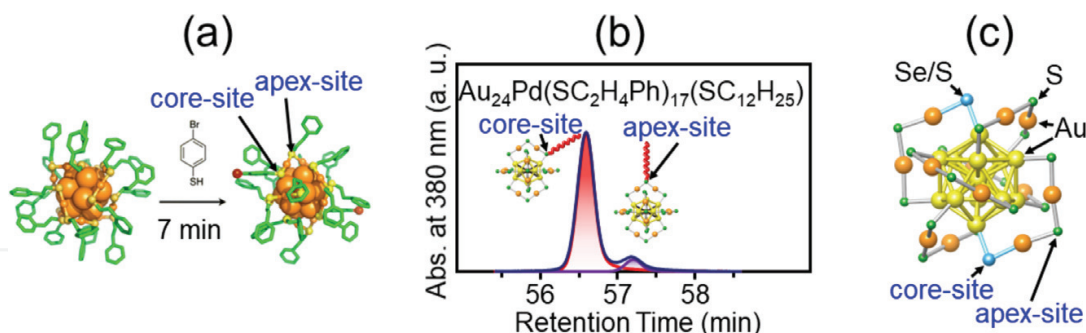


Figure 9. Preferential sites in ligand exchange reactions. (a) and (c) Geometrical structures of the products obtained from the reaction between $\text{Au}_{25}(\text{SC}_2\text{H}_4\text{Ph})_{18}$ and *para*-bromobenzenethiol and benzeneselenol, respectively. (b) Chromatogram of the product obtained from the reaction between $\text{Au}_{24}\text{Pd}(\text{SC}_2\text{H}_4\text{Ph})_{17}(\text{SC}_{12}\text{H}_{25})$ and dodecanethiol (these figures were adapted from Refs. [103, 104, 106]).

with *para*-bromobenzenethiol to ascertain which SR was more likely to be exchanged [103]. The results showed that $\text{Au}_{25}(\text{SC}_2\text{H}_4\text{Ph})_{16}(\text{p-BBT})_2$ (*p*-BBT = *para*-bromobenzenethiolate), in which the substitution had occurred at the core-site SR ligands, was obtained (**Figure 9(a)**), suggesting that the ligand exchange occurred at the core-site SR locations. However, this prior work did not determine whether other structures may have been present in the reaction mixture or not. For this reason, Niihori et al. employed reversed-phase high-performance liquid chromatography to allow the high-resolution separation of the coordination isomers generated by a similar reaction and estimated the distribution of isomers in the product. It was confirmed that the product mixture mainly contained a coordination isomer in which the core-site SR ligands had been substituted (**Figure 9(b)**) [104]. Fernando and Aikens performed density functional theory (DFT) calculations at approximately the same time, and the results indicated that ligand exchange was likely to occur at core-site SR ligands in $\text{Au}_{25}(\text{SR})_{18}$ [105]. These results demonstrated that ligand exchange preferentially proceeds at core-site SR ligands in $\text{Au}_{25}(\text{SC}_2\text{H}_4\text{Ph})_{18}$. The research by Hossain et al. has revealed that preferential exchange at core-site SR ligands also occurs in the reaction between $[\text{Au}_{25}(\text{SC}_2\text{H}_4\text{Ph})_{18}]^-$ and other chalcogenides (**Figure 9(c)**) [106].

6.2. Induction of quasi-isomerization

Studies have found that, in addition to ligand exchange, a change in geometry can also take place during reactions with thiol (RSH) (**Figure 8(b)**). This discovery originated from the prediction of the geometry of $\text{Au}_{24}(\text{SR})_{20}$ clusters. Specifically, Jin et al. synthesized $\text{Au}_{24}(\text{SC}_2\text{H}_4\text{Ph})_{20}$ in 2010 [107], after which Pei and coworkers predicted the geometry of these clusters via DFT calculations based on $\text{Au}_{24}(\text{SCH}_3)_{20}$ [108]. Thereafter, Jin et al. characterized $\text{Au}_{24}(\text{SCH}_2\text{Ph-}^t\text{Bu})_{20}$ ($\text{SCH}_2\text{Ph-}^t\text{Bu}$ = 4-*tert*-butylphenylmethanethiolate) by single-crystal X-ray structural analysis but found that the resulting structure was different from that predicted by Pei's group [109]. This discrepancy prompted Jiang et al. to study the geometric structures of $\text{Au}_{24}(\text{SR})_{20}$ clusters ($\text{R} = \text{CH}_3, \text{C}_2\text{H}_4\text{Ph}, \text{or } \text{CH}_2\text{Ph-}^t\text{Bu}$) using DFT, leading to the conclusion that the most stable structure of a $\text{Au}_{24}(\text{SR})_{20}$ cluster depends on the ligand [110]. At present, this theory has not been proven experimentally for $\text{Au}_{24}(\text{SR})_{20}$. However, in 2016, Jin et al. reported that exchanging the ligands of $\text{Au}_{28}(\text{SPh-}^t\text{Bu})_{20}$ ($\text{SPh-}^t\text{Bu}$ = 4-*tert*-butylbenzenethiolate) with cyclohexanethiolate ($\text{S-}c\text{-C}_6\text{H}_{11}$) altered the skeletal structure of the cluster (**Figure 10(a)**) [111].

This same work also demonstrated that exchanging the ligands of $\text{Au}_{28}(\text{S}-\text{C}-\text{C}_6\text{H}_{11})_{20}$ with $\text{SPh-}^t\text{Bu}$ regenerated the original geometry, meaning that the reaction was reversible (**Figure 10(a)**) [111]. Thus, it has recently been revealed that both ligand exchange and quasi-isomerization (as opposed to true isomerization because the ligand is different) can be induced for a particular $\text{Au}_n(\text{SR})_m$ cluster.

6.3. Induction of size transformation

Researches have also shown that the introduction of a significant structural deformation via ligand exchange can result in the formation of $\text{Au}_n(\text{SR})_m$ clusters with different chemical compositions (**Figure 8(c)**) [102]. An example is the reaction of $\text{Au}_{38}(\text{SC}_2\text{H}_4\text{Ph})_{24}$ clusters (**Figure 3(b)**) with $^t\text{Bu-PhSH}$ in solution, from which $\text{Au}_{36}(\text{SPh-}^t\text{Bu})_{24}$ was generated as the main product (yield ~90%) (**Figure 10(b)**) [112]. This outcome indicates that exchange with a ligand containing a bulky functional group can affect the chemical composition of the cluster.

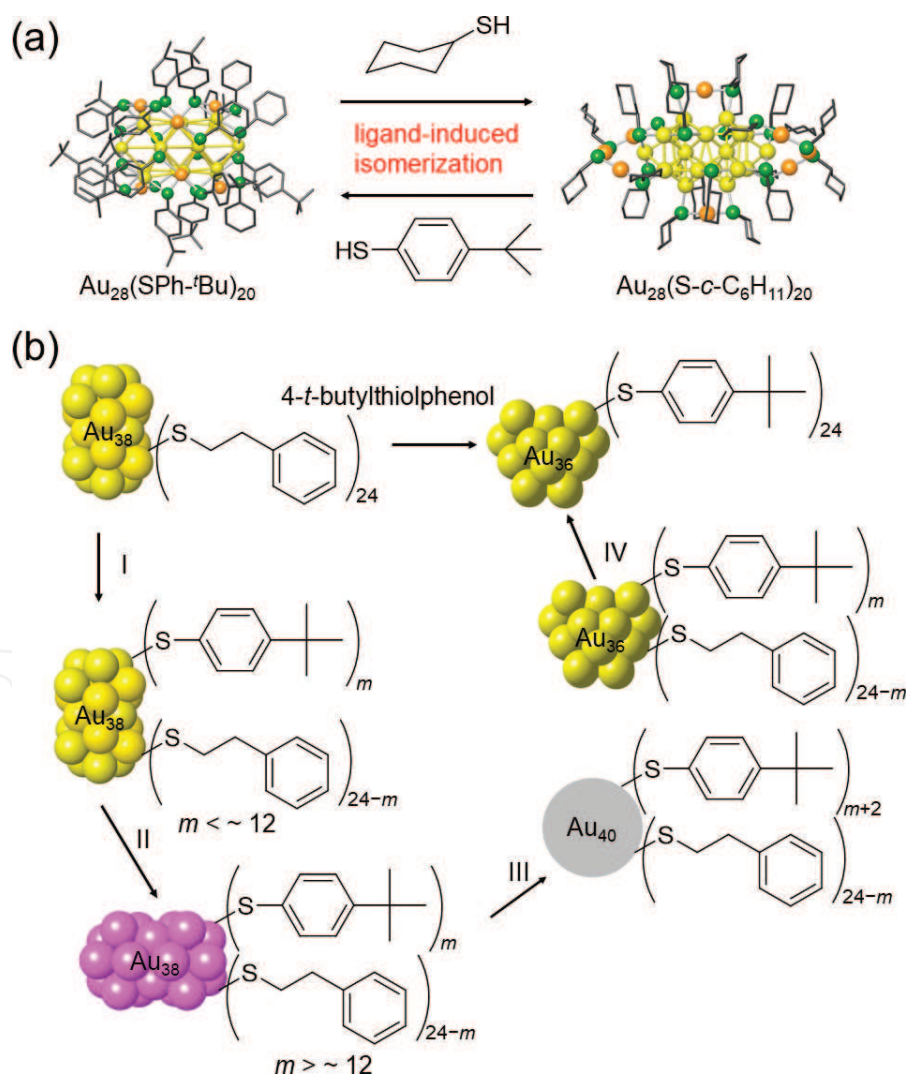


Figure 10. Examples of ligand exchange reactions, including (a) quasi-isomerization and (b) size transformation (these figures were adapted from Refs. [111, 112]).

Research regarding the mechanism of such reactions has also been conducted. Jin et al. found that the following four processes occur in the reaction between $\text{Au}_{38}(\text{SC}_2\text{H}_4\text{Ph})_{24}$ and $^t\text{Bu-PhSH}$: (I) ligand exchange, (II) structural distortion, (III) disproportionation, and (IV) size focusing conversion together with further ligand exchange (**Figure 10(b)**) [112]. In the first process, ligand exchange occurs without size or structural transformations, while the structural distortion of the resulting $\text{Au}_{38}(\text{SC}_2\text{H}_4\text{Ph})_{24-m}(\text{SPh-}^t\text{Bu})_m$ ($m > \sim 12$) is initiated in the second process. During the third process, one $\text{Au}_{38}(\text{SC}_2\text{H}_4\text{Ph})_{24-m}(\text{SPh-}^t\text{Bu})_m$ releases two gold atoms to form Au_{36} and another $\text{Au}_{38}(\text{SC}_2\text{H}_4\text{Ph})_{24-m}(\text{SPh-}^t\text{Bu})_m$ captures these two atoms and two free ligands to form $\text{Au}_{40}(\text{SC}_2\text{H}_4\text{Ph})_{24-m}(\text{SPh-}^t\text{Bu})_{m+2}$. In the final process, the $\text{Au}_{40}(\text{SC}_2\text{H}_4\text{Ph})_{24-m}(\text{SPh-}^t\text{Bu})_{m+2}$ begins to convert to Au_{36} , such that pure $\text{Au}_{36}(\text{SPh-}^t\text{Bu})_{24}$ is eventually obtained (**Figure 1(b)**). $\text{Au}_n(\text{SR})_m$ clusters such as $\text{Au}_{28}(\text{SPh-}^t\text{Bu})_{20}$, $\text{Au}_{36}(\text{SPh-}^t\text{Bu})_{24}$, and $\text{Au}_{36}(\text{S-}i\text{-C}_5\text{H}_9)_{24}$, none of which can be generated via direct synthesis at atomic precision, have also been synthesized in a size-selective manner by inducing this kind of structural deformation [102].

6.4. Relation between ligand structure and outcome

In this way, the outcomes are significantly affected by the bulkiness of the ligand in the ligand exchange reactions. Normally, ligand exchange with alkanethiol or $\text{PhC}_2\text{H}_4\text{SH}$ does not result in structural transformation, but simply leads to ligand exchange. Conversely, a bulky ligand such as $^t\text{Bu-PhSH}$ often leads to structural transformation. At present, there are no clear rules for predicting the final state of the deformed cluster (whether quasi-isomerization or size transformation). The final state seems to be related to the magnitude of the structural transformation and the possibility of isomeric structures with similar stabilities.

7. Summary

This chapter summarized common methods of fabricating $\text{Au}_n(\text{XR})_m$ clusters and surveyed the various geometric and electronic structures of these compounds, as well as their physical and chemical properties. Recent discoveries regarding ligand exchange reactions capable of enhancing the functionality of these clusters were also described. Although the precise synthesis of such clusters was first reported only 13 years ago at the time of writing, many studies regarding these clusters have been conducted in the interim, all of which have significantly improved our understanding of synthetic methods as well as the structures and functions of the clusters. It is expected that more information related to $\text{Au}_n(\text{XR})_m$ clusters will be gained on the basis of continuing research, leading to the readily synthesis of metal clusters with desired functions in the near future.

Acknowledgements

This work was partly supported by the Japan Society for the Promotion of Science (JSPS) KAKENHI (grant numbers JP16H04099, 16 K17480, and 17 K19040) and by the Scientific

Research on Innovative Areas (Coordination Asymmetry) (grant number 17H05385). Funding from the Takahashi Industrial and Economic Research Foundation, Futaba Electronics Memorial Foundation, Iwatani Naoji Foundation, Murata Science Foundation, and Ube Industries Foundation is also gratefully acknowledged. We thank Michael D. Judge, MSc, from Edanz Group (www.edanzediting.com/ac) for editing a draft of this manuscript.

Conflict of interest

There are no conflicts to declare.

Author details

Sakiat Hossain¹, Lakshmi V. Nair², Junta Inoue², Yuki Koyama², Wataru Kurashige² and Yuichi Negishi^{1,2*}

*Address all correspondence to: negishi@rs.kagu.tus.ac.jp

1 Photocatalysis International Research Center, Tokyo University of Science, Noda, Chiba, Japan

2 Department of Applied Chemistry, Faculty of Science, Tokyo University of Science, Tokyo, Japan

References

- [1] Corain B, Schmid G, Toshima N, editors. *Metal Nanoclusters in Catalysis and Materials Science: The Issue of Size Control*. 1st ed. Amsterdam: Elsevier; 2007. 470 p
- [2] McKenzie LC, Zaikova TO, Hutchison JE. Structurally similar triphenylphosphine-stabilized undecagolds, $\text{Au}_{11}(\text{PPh}_3)_7\text{Cl}_3$ and $[\text{Au}_{11}(\text{PPh}_3)_8\text{Cl}_2]\text{Cl}$, exhibit distinct ligand exchange pathways with glutathione. *Journal of the American Chemical Society*. 2014; **136**:13426-13435. DOI: 10.1021/ja5075689
- [3] Vollenbroek FA, Bour J, Velden JWA. Gold-phosphine cluster compounds. The reactions of $[\text{Au}_9\text{L}_8]^{3+}$ (L = PPh₃) with L, SCN⁻ and Cl⁻ to $[\text{Au}_8\text{L}_8]^{2+}$ ($\text{Au}_{11}\text{L}_8(\text{SCN})_2$)⁺ and $[\text{Au}_{11}\text{L}_8\text{Cl}_2]^+$. *Recueil des Travaux Chimiques des Pays-Bas*. 1980;**99**:137-141. DOI: 10.1002/recl.19800990410
- [4] Schulz-Dobrick M, Jansen M. Characterization of gold clusters by crystallization with polyoxometalates: The intercluster compounds $[\text{Au}_9(\text{dpph})_4][\text{Mo}_8\text{O}_{26}]$, $[\text{Au}_9(\text{dpph})_4][\text{PW}_{12}\text{O}_{40}]$ and $[\text{Au}_{11}(\text{PPh}_3)_8\text{Cl}_2]_2[\text{W}_6\text{O}_{19}]$. *Zeitschrift für anorganische und allgemeine Chemie*. 2007;**633**:2326-2331. DOI: 10.1002/zaac.200700210

- [5] Woehrle GH, Warner MG, Hutchison JE. Ligand exchange reactions yield subnanometer, thiol-stabilized gold particles with defined optical transitions. *The Journal of Physical Chemistry B*. 2002;**106**:9979-9981. DOI: 10.1021/jp025943s
- [6] Yang Y, Chen S. Surface manipulation of the electronic energy of subnanometer-sized gold clusters: An electrochemical and spectroscopic investigation. *Nano Letters*. 2003;**3**:75-79. DOI: 10.1021/nl025809j
- [7] Shichibu Y, Negishi Y, Tsukuda T, Teranishi T. Large-scale synthesis of thiolated Au₂₅ clusters via ligand exchange reactions of phosphine-stabilized Au₁₁ clusters. *Journal of the American Chemical Society*. 2005;**127**:13464-13465. DOI: 10.1021/ja053915s
- [8] Liu Y, Tsunoyama H, Akita T, Tsukuda T. Preparation of ~1 nm gold clusters confined within mesoporous silica and microwave-assisted catalytic application for alcohol oxidation. *The Journal of Physical Chemistry C*. 2009;**113**:13457-13461. DOI: 10.1021/jp904700p
- [9] Walter M, Akola J, Lopez-Acevedo O, Jadzinsky PD, Calero G, Ackerson CJ, Whetten RL, Grönbeck H, Häkkinen H. A unified view of ligand-protected gold clusters as superatom complexes. *Proceedings of the National Academy of Sciences of the United States of America*. 2008;**105**:9157-9162. DOI: 10.1073/pnas.0801001105
- [10] Briant CE, Theobald BRC, White JW, Bell LK, Mingos DMP, Welch AJ. Synthesis and X-ray structural characterization of the centred icosahedral gold cluster compound [Au₁₃(PMe₂Ph)₁₀Cl₂](PF₆)₃; the realization of a theoretical prediction. *Journal of the Chemical Society, Chemical Communications*. 1981:201-202. DOI: 10.1039/C39810000201
- [11] Teo B, Shi X, Zhang H. Pure gold cluster of 1:9:9:1:9:9:1 layered structure: A novel 39-metal-atom cluster [(Ph₃P)₁₄Au₃₉Cl₆]Cl₂ with an interstitial gold atom in a hexagonal antiprismatic cage. *Journal of the American Chemical Society*. 1992;**114**:2743-2745. DOI: 10.1021/ja00033a073
- [12] Schmid G, Pfeil R, Boese R, Bandermann F, Meyer S, Calis GHM, Velden JWA. Au₅₅[P(C₆H₅)₃]₁₂Cl₆ - a gold cluster of an exceptional size. *Chemische Berichte-Recueil*. 1981;**114**:3634-3642. DOI: 10.1002/cber.19811141116
- [13] Schmid G. Large clusters and colloids. Metals in the embryonic state. *Chemical Reviews*. 1992;**92**:1709-1727. DOI: 10.1021/cr00016a002
- [14] Boyen HG, Kästle G, Weigl F, Koslowski B, Dietrich C, Ziemann P, Spatz JP, Riethmüller S, Hartmann C, Möller M, Schmid G, Garnier MG, Oelhafen P. Oxidation-resistant gold-55 clusters. *Science*. 2002;**297**:1533-1536. DOI: 10.1126/science.1076248
- [15] Inomata T, Konishi K. Gold nanocluster confined within a cage: Template-directed formation of a hexaporphyrin cage and its confinement capability. *Chemical Communications*. 2003:1282-1283. DOI: 10.1039/B302609D
- [16] Balasubramanian R, Guo R, Mills AJ, Murray RW. Reaction of Au₅₅(PPh₃)₁₂Cl₆ with thiols yields thiolate monolayer protected Au₇₅ clusters. *Journal of the American Chemical Society*. 2005;**127**:8126-8132. DOI: 10.1021/ja050793v

- [17] Brust M, Walker M, Bethell D, Schiffrin DJ, Whyman R. Synthesis of thiol-derivatised gold nanoparticles in a two-phase liquid–liquid system. *Journal of the Chemical Society, Chemical Communications*. 1994:801-802. DOI: 10.1039/C39940000801
- [18] Tsukuda T. Toward an atomic-level understanding of size-specific properties of protected and stabilized gold clusters. *Bulletin of the Chemical Society of Japan*. 2012;**85**: 151-168. DOI: 10.1246/bcsj.20110227
- [19] Whetten RL, Shafiqullin MN, Khoury JT, Schaaff TG, Vezmar I, Alvarez MM, Wilkinson A. Crystal structures of molecular gold nanocrystal arrays. *Accounts of Chemical Research*. 1999;**32**:397-406. DOI: 10.1021/ar970239t
- [20] Parker JF, Fields-Zinna CA, Murray RW. The story of a monodisperse gold nanoparticle: Au₂₅L₁₈. *Accounts of Chemical Research*. 2010;**43**:1289-1296. DOI: 10.1021/ar100048c
- [21] Murray RW. Nanoelectrochemistry: Metal nanoparticles, nanoelectrodes, and nanopores. *Chemical Reviews*. 2008;**108**:2688-2720. DOI: 10.1021/cr068077e
- [22] Li G, Jin R. Atomically precise gold nanoclusters as new model catalysts. *Accounts of Chemical Research*. 2013;**46**:1749-1758. DOI: 10.1021/ar300213z
- [23] Qian H, Zhu M, Wu Z, Jin R. Quantum sized gold nanoclusters with atomic precision. *Accounts of Chemical Research*. 2012;**45**:1470-1479. DOI: 10.1021/ar200331z
- [24] Dass A. Nano-scaling law: Geometric foundation of thiolated gold nanomolecules. *Nanoscale*. 2012;**4**:2260-2263. DOI: 10.1039/c2nr11749e
- [25] Negishi Y, Kurashige W, Niihori Y, Nobusada K. Toward the creation of stable, functionalized metal clusters. *Physical Chemistry Chemical Physics*. 2013;**15**:18736-18751. DOI: 10.1039/c3cp52837e
- [26] Negishi Y. Toward the creation of functionalized metal nanoclusters and highly active photocatalytic materials using thiolate-protected magic gold clusters. *Bulletin of the Chemical Society of Japan*. 2014;**87**:375-389. DOI: 10.1246/bcsj.20130288
- [27] Luo Z, Nachammai V, Zhang B, Yan N, Leong DT, Jiang DE, Xie J. Toward understanding the growth mechanism: Tracing all stable intermediate species from reduction of Au(I)–thiolate complexes to evolution of Au₂₅ nanoclusters. *Journal of the American Chemical Society*. 2014;**136**:10577-10580. DOI: 10.1021/ja505429f
- [28] Häkkinen H. The gold–sulfur interface at the nanoscale. *Nature Chemistry*. 2012;**4**: 443-455. DOI: 10.1038/nchem.1352
- [29] Zhu M, Aikens CM, Hollander FJ, Schatz GC, Jin R. Correlating the crystal structure of a thiol-protected Au₂₅ cluster and optical properties. *Journal of the American Chemical Society*. 2008;**130**:5883-5885. DOI: 10.1021/ja801173r
- [30] Qian H, Eckenhoff WT, Zhu Y, Pintauer T, Jin R. Total structure determination of thiolate-protected Au₃₈ nanoparticles. *Journal of the American Chemical Society*. 2010; **132**:8280-8281. DOI: 10.1021/ja103592z

- [31] Pei Y, Zeng XC. Investigating the structural evolution of thiolate protected gold clusters from first-principles. *Nanoscale*. 2012;**4**:4054-4072. DOI: 10.1039/c2nr30685a
- [32] Zhang P. X-ray spectroscopy of gold–thiolate nanoclusters. *The Journal of Physical Chemistry C*. 2014;**118**:25291-25299. DOI: 10.1021/jp507739u
- [33] Jiang DE, Kühn M, Tang Q, Weigend F. Superatomic orbitals under spin–orbit coupling. *The Journal of Physical Chemistry Letters*. 2014;**5**:3286-3289. DOI: 10.1021/jz501745z
- [34] Jadzinsky PD, Calero G, Ackerson CJ, Bushnell DA, Kornberg RD. Structure of a thiol monolayer-protected gold nanoparticle at 1.1 Å resolution. *Science*. 2007;**318**:430-433. DOI: 10.1126/science.1148624
- [35] Knoppe S, Wong OA, Malola S, Häkkinen H, Bürgi T, Verbiest T, Ackerson CJ. Chiral phase transfer and enantioenrichment of thiolate-protected Au₁₀₂ clusters. *Journal of the American Chemical Society*. 2014;**136**:4129-4132. DOI: 10.1021/ja500809p
- [36] Dolamic I, Knoppe S, Dass A, Bürgi T. First enantioseparation and circular dichroism spectra of Au₃₈ clusters protected by achiral ligands. *Nature Communications*. 2012;**3**:798. DOI: 10.1038/ncomms1802
- [37] Udayabhaskararao T, Pradeep T. New protocols for the synthesis of stable Ag and Au nanocluster molecules. *The Journal of Physical Chemistry Letters*. 2013;**4**:1553-1564. DOI: 10.1021/jz400332g
- [38] Dainese T, Antonello S, Gascón JA, Pan F, Perera NV, Ruzzi M, Venzo A, Zoleo A, Rissanen K, Maran F. Au₂₅(SEt)₁₈, a nearly naked thiolate-protected Au₂₅ cluster: Structural analysis by single crystal X-ray crystallography and electron nuclear double resonance. *ACS Nano*. 2014;**8**:3904-3912. DOI: 10.1021/nn500805n
- [39] Li Y, Zaluzhna O, Tong YYJ. Critical role of water and the structure of inverse micelles in the Brust–Schiffrin synthesis of metal nanoparticles. *Langmuir*. 2011;**27**:7366-7370. DOI: 10.1021/la201158v
- [40] Kwak K, Kumar SS, Pyo K, Lee D. Ionic liquid of a gold nanocluster: A versatile matrix for electrochemical biosensors. *ACS Nano*. 2014;**8**:671-679. DOI: 10.1021/nn4053217
- [41] Negishi Y, Kurashige W, Kamimura U. Isolation and structural characterization of an octaneselenolate-protected Au₂₅ cluster. *Langmuir*. 2011;**27**:12289-12292. DOI: 10.1021/la203301p
- [42] Kurashige W, Yamaguchi M, Nobusada K, Negishi Y. Ligand-induced stability of gold nanoclusters: Thiolate versus selenolate. *The Journal of Physical Chemistry Letters*. 2012;**3**:2649-2652. DOI: 10.1021/jz301191t
- [43] Kurashige W, Yamazoe S, Kanehira K, Tsukuda T, Negishi Y. Selenolate-protected Au₃₈ nanoclusters: Isolation and structural characterization. *The Journal of Physical Chemistry Letters*. 2013;**4**:3181-3185. DOI: 10.1021/jz401770y

- [44] Kurashige W, Munakata K, Nobusada K, Negishi Y. Synthesis of stable $\text{Cu}_n\text{Au}_{25-n}$ nanoclusters ($n = 1-9$) using selenolate ligands. *Chemical Communications*. 2013;**49**: 5447-5449. DOI: 10.1039/c3cc41210e
- [45] Kurashige W, Yamazoe S, Yamaguchi M, Nishido K, Nobusada K, Tsukuda T, Negishi Y. Au_{25} clusters containing unoxidized tellurolates in the ligand shell. *The Journal of Physical Chemistry Letters*. 2014;**5**:2072-2076. DOI: 10.1021/jz500901f
- [46] Meng X, Xu Q, Wang S, Zhu M. Ligand-exchange synthesis of selenophenolate-capped Au_{25} nanoclusters. *Nanoscale*. 2012;**4**:4161-4165. DOI: 10.1039/c2nr30272a
- [47] Song Y, Wang S, Zhang J, Kang X, Chen S, Li P, Sheng H, Zhu M. Crystal structure of selenolate-protected $\text{Au}_{24}(\text{SeR})_{20}$ nanocluster. *Journal of the American Chemical Society*. 2014;**136**:2963-2965. DOI: 10.1021/ja413114z
- [48] Song Y, Zhong J, Yang S, Wang S, Cao T, Zhang J, Li P, Hu D, Pei Y, Zhu M. Crystal structure of $\text{Au}_{25}(\text{SePh})_{18}$ nanoclusters and insights into their electronic, optical and catalytic properties. *Nanoscale*. 2014;**6**:13977-13985. DOI: 10.1039/c4nr04631e
- [49] Song Y, Abroshan H, Chai J, Kang X, Kim HJ, Zhu M, Jin R. Molecular-like transformation from PhSe-protected Au_{25} to Au_{23} nanocluster and its application. *Chemistry of Materials*. 2017;**29**:3055-3061. DOI: 10.1021/acs.chemmater.7b00058
- [50] Song Y, Cao T, Deng H, Zhu X, Li P, Zhu M. Kinetically controlled, high-yield, direct synthesis of $[\text{Au}_{25}(\text{SePh})_{18}]^- \text{TOA}^+$. *Science China*. 2014;**57**:1218-1224. DOI: 10.1007/s11426-014-5071-5
- [51] Xu Q, Wang S, Liu Z, Xu G, Meng X, Zhu M. Synthesis of selenolate-protected $\text{Au}_{18}(\text{SeC}_6\text{H}_5)_{14}$ nanoclusters. *Nanoscale*. 2013;**5**:1176-1182. DOI: 10.1039/c2nr33466f
- [52] Maity P, Takano S, Yamazoe S, Wakabayashi T, Tsukuda T. Binding motif of terminal alkynes on gold clusters. *Journal of the American Chemical Society*. 2013;**135**:9450-9457. DOI: 10.1021/ja401798z
- [53] Wan XK, Tang Q, Yuan SF, Jiang DE, Wang QM. Au_{19} nanocluster featuring a V-shaped alkynyl-gold motif. *Journal of the American Chemical Society*. 2015;**137**:652-655. DOI: 10.1021/ja512133a
- [54] Lei Z, Wan XK, Yuan SF, Wang JQ, Wang QM. Alkynyl-protected gold and gold-silver nanoclusters. *Dalton Transactions*. 2017;**46**:3427-3434. DOI: 10.1039/c6dt04763g
- [55] Shichibu Y, Negishi Y, Watanabe T, Chaki NK, Kawaguchi H, Tsukuda T. Biicosahedral gold clusters $[\text{Au}_{25}(\text{PPh}_3)_{10}(\text{SC}_n\text{H}_{2n+1})_5\text{Cl}_2]^{2+}$ ($n = 2-18$): A stepping stone to cluster-assembled materials. *The Journal of Physical Chemistry C*. 2007;**111**:7845-7847. DOI: 10.1021/jp073101t
- [56] Koshevoy IO, Chang YC, Chen YA, Karttunen AJ, Grachova EV, Tunik SP, Jänis J, Pakkanen TA, Chou PT. Luminescent gold(I) alkynyl clusters stabilized by flexible diphosphine ligands. *Organometallics*. 2014;**33**:2363-2371. DOI: 10.1021/om5002952

- [57] Song Y, Jin S, Kang X, Xiang J, Deng H, Yu H, Zhu M. How a single electron affects the properties of the "non-superatom" Au₂₅ nanoclusters. *Chemistry of Materials*. 2016; **28**:2609-2617. DOI: 10.1021/acs.chemmater.5b04655
- [58] Kobayashi N, Kamei Y, Shichibu Y, Konishi K. Protonation-induced chromism of pyridylethynyl-appended [core+exo]-type Au₈ clusters. Resonance-coupled electronic perturbation through π -conjugated group. *Journal of the American Chemical Society*. 2013; **135**:16078-16081. DOI: 10.1021/ja4099092
- [59] Kang X, Song Y, Deng H, Zhang J, Liu B, Pan C, Zhu M. Ligand-induced change of the crystal structure and enhanced stability of the Au₁₁ nanocluster. *RSC Advance*. 2015; **5**:66879-66885. DOI: 10.1039/c5ra11674k
- [60] Song Y, Huang T, Murray RW. Heterophase ligand exchange and metal transfer between monolayer protected clusters. *Journal of the American Chemical Society*. 2003; **125**:11694-11701. DOI: 10.1021/ja0355731
- [61] Lee D, Donkers RL, Wang G, Harper AS, Murray RW. Electrochemistry and optical absorbance and luminescence of molecule-like Au₃₈ nanoparticles. *Journal of the American Chemical Society*. 2004; **126**:6193-6199. DOI: 10.1021/ja049605b
- [62] Guo R, Song Y, Wang G, Murray RW. Does core size matter in the kinetics of ligand exchanges of monolayer-protected Au clusters? *Journal of the American Chemical Society*. 2005; **127**:2752-2757. DOI: 10.1021/ja044638c
- [63] Hostetler MJ, Templeton AC, Murray RW. Dynamics of place-exchange reactions on monolayer-protected gold cluster molecules. *Langmuir*. 1999; **15**:3782-3789. DOI: 10.1021/la981598f
- [64] Tracy JB, Crowe MC, Parker JF, Hampe O, Fields-Zinna CA, Dass A, Murray RW. Electrospray ionization mass spectrometry of uniform and mixed monolayer nanoparticles: Au₂₅[S(CH₂)₂Ph]₁₈ and Au₂₅[S(CH₂)₂Ph]_{18-x}(SR)_x. *Journal of the American Chemical Society*. 2007; **129**:16209-16215. DOI: 10.1021/ja076621a
- [65] Song Y, Murray RW. Dynamics and extent of ligand exchange depend on electronic charge of metal nanoparticles. *Journal of the American Chemical Society*. 2002; **124**:7096-7102. DOI: 10.1021/ja0174985
- [66] Niihori Y, Hossain S, Kumar B, Nair LV, Kurashige W, Negishi Y. Perspective: Exchange reactions in thiolate-protected metal clusters. *APL Materials*. 2017; **5**:053201. DOI: 10.1063/1.4978373
- [67] Niihori Y, Hossain S, Sharma S, Kumar B, Kurashige W, Negishi Y. Understanding and practical use of ligand and metal exchange reactions in thiolate-protected metal clusters to synthesize controlled metal clusters. *The Chemical Record*. 2017; **17**:473-484. DOI: 10.1002/tcr.201700002
- [68] Wu Z, Suhan J, Jin R. One-pot synthesis of atomically monodisperse, thiol-functionalized Au₂₅ nanoclusters. *Journal of Materials Chemistry*. 2009; **19**:622-626. DOI: 10.1039/b815983a

- [69] Schaaff TG, Whetten RL. Giant gold–glutathione cluster compounds: Intense optical activity in metal-based transitions. *The Journal of Physical Chemistry B*. 2000;**104**:2630-2641. DOI: 10.1021/jp993691y
- [70] Negishi Y, Takasugi Y, Sato S, Yao H, Kimura K, Tsukuda T. Magic-numbered Au_{*n*} clusters protected by glutathione monolayers (*n* = 18, 21, 25, 28, 32, 39): Isolation and spectroscopic characterization. *Journal of the American Chemical Society*. 2004;**126**:6518-6519. DOI: 10.1021/ja0483589
- [71] Negishi Y, Nobusada K, Tsukuda T. Glutathione-protected gold clusters revisited: Bridging the gap between gold(I)–thiolate complexes and thiolate-protected gold nanocrystals. *Journal of the American Chemical Society*. 2005;**127**:5261-5270. DOI: 10.1021/ja042218h
- [72] Tsukuda T, Häkkinen H, editors. *Protected Metal Clusters: From Fundamentals to Applications*. 1st ed. Amsterdam: Elsevier; 2015. 372 p
- [73] Wolfe RL, Murray RW. Analytical evidence for the monolayer-protected cluster Au₂₂₅[(S(CH₂)₅CH₃)]₇₅. *Analytical Chemistry*. 2006;**78**:1167-1173. DOI: 10.1021/ac051533z
- [74] Choi MMF, Douglas AD, Murray RW. Ion-pair chromatographic separation of water-soluble gold monolayer-protected clusters. *Analytical Chemistry*. 2006;**78**:2779-2785. DOI: 10.1021/ac052167m
- [75] Negishi Y, Nakazaki T, Malola S, Takano S, Niihori Y, Kurashige W, Yamazoe S, Tsukuda T, Häkkinen H. A critical size for emergence of nonbulk electronic and geometric structures in dodecanethiolate-protected Au clusters. *Journal of the American Chemical Society*. 2015;**137**:1206-1212. DOI: 10.1021/ja5109968
- [76] Niihori Y, Matsuzaki M, Uchida C, Negishi Y. Advanced use of high-performance liquid chromatography for synthesis of controlled metal clusters. *Nanoscale*. 2014;**6**:7889-7896. DOI: 10.1039/c4nr01144a
- [77] Black DM, Bhattarai N, Bach SBH, Whetten RL. Selection and identification of molecular gold clusters at the nano(gram) scale: Reversed phase HPLC–ESI–MS of a mixture of Au-peth MPCs. *The Journal of Physical Chemistry Letters*. 2016;**7**:3199-3205. DOI: 10.1021/acs.jpcllett.6b01403
- [78] Negishi Y, Chaki NK, Shichibu Y, Whetten RL, Tsukuda T. Origin of magic stability of thiolated gold clusters: A case study on Au₂₅(SC₆H₁₃)₁₈. *Journal of the American Chemical Society*. 2007;**129**:11322-11323. DOI: 10.1021/ja073580+
- [79] Chaki NK, Negishi Y, Tsunoyama H, Shichibu Y, Tsukuda T. Ubiquitous 8 and 29 kDa gold: Alkanethiolate cluster compounds: Mass-spectrometric determination of molecular formulas and structural implications. *Journal of the American Chemical Society*. 2008;**130**:8608-8610. DOI: 10.1021/ja8005379
- [80] Schaaff TG, Whetten RL. Controlled etching of Au:SR cluster compounds. *The Journal of Physical Chemistry B*. 1999;**103**:9394-9396. DOI: 10.1021/jp993229d
- [81] Shichibu Y, Negishi Y, Tsunoyama H, Kanehara M, Teranishi T, Tsukuda T. Extremely high stability of glutathionate-protected Au₂₅ clusters against core etching. *Small*. 2007;**3**:835-839. DOI: 10.1002/sml.200600611

- [82] Jin R, Qian H, Wu Z, Zhu Y, Zhu M, Mohanty A, Garg N. Size focusing: A methodology for synthesizing atomically precise gold nanoclusters. *The Journal of Physical Chemistry Letters*. 2010;**1**:2903-2910. DOI: 10.1021/jz100944k
- [83] Zeng C, Chen Y, Das A, Jin R. Transformation chemistry of gold nanoclusters: From one stable size to another. *The Journal of Physical Chemistry Letters*. 2015;**6**:2976-2986. DOI: 10.1021/acs.jpcclett.5b01150
- [84] Häkkinen H, Barnett RN, Landman U. Electronic structure of passivated Au₃₈(SCH₃)₂₄ nanocrystal. *Physical Review Letters*. 1999;**82**:3264-3267. DOI: 10.1103/PhysRevLett.82.3264
- [85] Zeng C, Qian H, Li T, Li G, Rosi NL, Yoon B, Barnett RN, Whetten RL, Landman U, Jin R. Total structure and electronic properties of the gold nanocrystal Au₃₆(SR)₂₄. *Angewandte Chemie International Edition*. 2012;**51**:13114-13118. DOI: 10.1002/anie.201207098
- [86] Dass A, Theivendran S, Nimmala PR, Kumara C, Jupally VR, Fortunelli A, Sementa L, Barcaro G, Zuo X, Noll BC. Au₁₃₃(SPh-^tBu)₅₂ nanomolecules: X-ray crystallography, optical, electrochemical, and theoretical analysis. *Journal of the American Chemical Society*. 2015;**137**:4610-4613. DOI: 10.1021/ja513152h
- [87] Das A, Li T, Nobusada K, Zeng C, Rosi NL, Jin R. Nonsuperatomic [Au₂₃(SC₆H₁₁)₁₆]⁻ nanocluster featuring bipyramidal Au₁₅ kernel and trimeric Au₃(SR)₄ motif. *Journal of the American Chemical Society*. 2013;**135**:18264-18267. DOI: 10.1021/ja409177s
- [88] Heaven MW, Dass A, White PS, Holt KM, Murray RW. Crystal structure of the gold nanoparticle [N(C₈H₁₇)₄][Au₂₅(SCH₂CH₂Ph)₁₈]. *Journal of the American Chemical Society*. 2008;**130**:3754-3755. DOI: 10.1021/ja800561b
- [89] Pohjolainen E, Häkkinen H, Clayborne A. The role of the anchor atom in the ligand of the monolayer-protected Au₂₅(XR)₁₈⁻ nanocluster. *The Journal of Physical Chemistry C*. 2015;**119**:9587-9594. DOI: 10.1021/acs.jpcc.5b01068
- [90] Kumar S, Jin R. Water-soluble Au₂₅(Capt)₁₈ nanoclusters: Synthesis, thermal stability, and optical properties. *Nanoscale*. 2012;**4**:4222-4227. DOI: 10.1039/C2NR30833A
- [91] Lin SY, Chen NT, Sum SP, Lo LW, Yang CS. Ligand exchanged photoluminescent gold quantum dots functionalized with leading peptides for nuclear targeting and intracellular imaging. *Chemical Communications*. 2008:4762-4764. DOI: 10.1039/b808207c
- [92] Kano S, Azuma Y, Kanehara M, Teranishi T, Majima Y. Room-temperature coulomb blockade from chemically synthesized Au nanoparticles stabilized by acid-base interaction. *Applied Physics Express*. 2010;**3**:105003. DOI: 10.1143/APEX.3.105003
- [93] Lopez-Acevedo O, Tsunoyama H, Tsukuda T, Häkkinen H, Aikens CM. Chirality and electronic structure of the thiolate-protected Au₃₈ nanocluster. *Journal of the American Chemical Society*. 2010;**132**:8210-8218. DOI: 10.1021/ja102934q
- [94] Malola S, Lehtovaara L, Knoppe S, Hu KJ, Palmer RE, Bürgi T, Häkkinen H. Au₄₀(SR)₂₄ cluster as a chiral dimer of 8-electron superatoms: Structure and optical properties. *Journal of the American Chemical Society*. 2012;**134**:19560-19563. DOI: 10.1021/ja309619n

- [95] Knoppe S, Bürgi T. Chirality in thiolate-protected gold clusters. *Accounts of Chemical Research*. 2014;**47**:1318-1326. DOI: 10.1021/ar400295d
- [96] Noyori R. Asymmetric catalysis: Science and opportunities (nobel lecture). *Angewandte Chemie International Edition*. 2002;**41**:2008-2022. DOI: 10.1002/1521-3773(20020617)41:12<2008::AID-ANIE2008>3.0.CO;2-4
- [97] de la Llave E, Scherlis DA. Selenium-based self-assembled monolayers: The nature of adsorbate–surface interactions. *Langmuir*. 2010;**26**:173-178. DOI: 10.1021/la903660y
- [98] Szelagowska-Kunstman K, Cyganik P, Schüpbach B, Terfort A. Relative stability of thiol and selenol based SAMs on Au(111)—exchange experiments. *Physical Chemistry Chemical Physics*. 2010;**12**:4400-4406. DOI: 10.1039/b923274p
- [99] Kurashige W, Niihori Y, Sharma S, Negishi Y. Precise synthesis, functionalization and application of thiolate-protected gold clusters. *Coordination Chemistry Reviews*. 2016; **320-321**:238-250. DOI: 10.1016/j.ccr.2016.02.013
- [100] Romashov LV, Ananikov VP. Self-assembled selenium monolayers: From nanotechnology to materials science and adaptive catalysis. *Chemistry—A European Journal*. 2013;**19**:17640-17660. DOI: 10.1002/chem.201302115
- [101] Yokota K, Taniguchi M, Kawai T. Control of the electrode–molecule interface for molecular devices. *Journal of the American Chemical Society*. 2007;**129**:5818-5819. DOI: 10.1021/ja071365n
- [102] Jin R, Zeng C, Zhou M, Chen Y. Atomically precise colloidal metal nanoclusters and nanoparticles: Fundamentals and opportunities. *Chemical Reviews*. 2016;**116**:10346-10413. DOI: 10.1021/acs.chemrev.5b00703
- [103] Ni TW, Tofanelli MA, Phillips BD, Ackerson CJ. Structural basis for ligand exchange on Au₂₅(SR)₁₈. *Inorganic Chemistry*. 2014;**53**:6500-6502. DOI: 10.1021/ic5010819
- [104] Niihori Y, Kikuchi Y, Kato A, Matsuzaki M, Negishi Y. Understanding ligand-exchange reactions on thiolate-protected gold clusters by probing isomer distributions using reversed-phase high-performance liquid chromatography. *ACS Nano*. 2015;**9**:9347-9356. DOI: 10.1021/acs.nano.5b03435
- [105] Fernando A, Aikens CM. Ligand exchange mechanism on thiolate monolayer protected Au₂₅(SR)₁₈ nanoclusters. *The Journal of Physical Chemistry C*. 2015;**119**:20179-20187. DOI: 10.1021/acs.jpcc.5b06833
- [106] Hossain S, Kurashige W, Wakayama S, Kumar B, Nair LV, Niihori Y, Negishi Y. Ligand exchange reactions in thiolate-protected Au₂₅ nanoclusters with selenolates or tellurolates: Preferential exchange sites and effects on electronic structure. *The Journal of Physical Chemistry C*. 2016;**120**:25861-25869. DOI: 10.1021/acs.jpcc.6b08636
- [107] Zhu M, Qian H, Jin R. Thiolate-protected Au₂₄(SC₂H₄Ph)₂₀ nanoclusters: Superatoms or not? *The Journal of Physical Chemistry Letters*. 2010;**1**:1003-1007. DOI: 10.1021/jz100133n
- [108] Pei Y, Pal R, Liu C, Gao Y, Zhang Z, Zeng XC. Interlocked catenane-like structure predicted in Au₂₄(SR)₂₀: Implication to structural evolution of thiolated gold clusters

from homoleptic gold(I) thiolates to core-stacked nanoparticles. *Journal of the American Chemical Society*. 2012;**134**:3015-3024. DOI: 10.1021/ja208559y

- [109] Das A, Li T, Li G, Nobusada K, Zeng C, Rosi NL, Jin R. Crystal structure and electronic properties of a thiolate-protected Au₂₄ nanocluster. *Nanoscale*. 2014;**6**:6458-6462. DOI: 10.1039/c4nr01350f
- [110] Tang Q, Ouyang R, Tian Z, Jiang DE. The ligand effect on the isomer stability of Au₂₄(SR)₂₀ clusters. *Nanoscale*. 2015;**7**:2225-2229. DOI: 10.1039/c4nr05826g
- [111] Chen Y, Liu C, Tang Q, Zeng C, Higaki T, Das A, Jiang DE, Rosi NL, Jin R. Isomerism in Au₂₈(SR)₂₀ nanocluster and stable structures. *Journal of the American Chemical Society*. 2016;**138**:1482-1485. DOI: 10.1021/jacs.5b12094
- [112] Zeng C, Liu C, Pei Y, Jin R. Thiol ligand-induced transformation of Au₃₈(SC₂H₄Ph)₂₄ to Au₃₆(SPh-*t*-Bu)₂₄. *ACS Nano*. 2013;**7**:6138-6145. DOI: 10.1021/nm401971g

IntechOpen